ELSEVIER

Contents lists available at ScienceDirect

Journal of Manufacturing Processes

journal homepage: www.elsevier.com/locate/manpro





Effects of surface coating materials on cutting forces and ductile-to-brittle transition in orthogonal cutting of monocrystalline sapphire

Hae-Sung Yoon a,b, Suk Bum Kwon, Ji-Hwan Kim, Sung-Hoon Ahn, Sangkee Min, Sangkee M

- ^a School of Aerospace and Mechanical Engineering, Korea Aerospace University, Gyeonggi-do, Republic of Korea
- ^b Department of Smart Air Mobility, Korea Aerospace University, Gyeonggi-do, Republic of Korea
- ^c Department of Mechanical Engineering, University of Wisconsin-Madison, WI, USA
- d Department of Mechanical Engineering, Seoul National University, Seoul, Republic of Korea

ARTICLE INFO

Keywords: Machinability Ceramic Ductile-regime cutting Coating Ultra-precision machining

ABSTRACT

Ductile regime cutting has been studied to process brittle materials without cracking. The predominant material response during cutting can be tuned to the ductile range under certain conditions. This study aims to explore and reveal the effects of workpiece surface coatings on promoting the ductile cutting regime. Despite of several attempts on applying surface coatings, the effects of coating properties on material behaviors and cutting forces are not yet well-understood. Here, the effects of surface coatings on the cutting forces during ductile regime cutting of monocrystalline sapphire were investigated from the perspectives of types of coating materials and crystal orientation. Flexible elastomers, hard coatings, and a lubricant were applied to the surface, and the cutting force behaviors were observed. Coatings effectively promoted ductile cutting regime, but the effects varied by coating type and crystal orientation. The cutting forces and ductile cutting regime were significantly influenced by types of coating materials and dominant deformation/fracture mechanisms of sapphire crystal. The machining characteristics were analyzed based on the modified slip-fracture model; this explained the varying effects per different cutting direction. This study aids identification of effective coatings under various cutting conditions and is expected to contribute to wider utilization of ductile regime cutting in processing of brittle materials.

1. Introduction

Processing of engineering ceramics has been actively investigated thanks to their high level of hardness and corrosion resistance [1]. For example, monocrystalline sapphire has been widely utilized in the optics and semiconductor industries owing to its high chemical stability and optical transparency [2]. One of the critical issues in the processing of ceramics is their brittleness. During the shaping by mechanical machining, cracks likely occur and propagate [3], causing significant surface and subsurface damage. Subsurface damage can be up to a few times of processing depth [4]. Studies have been conducted to achieve high surface integrity mostly in abrasive processes [5] as well as to improve productivity of processes.

Considering this, ductile regime cutting has been studied to process ceramic materials without surface cracking. The predominant material

response during cutting can be tuned to the ductile range under certain conditions [6]. Ultra-precision machining has been used to observe the transition of the dominant material response, so-called brittle-to-ductile or ductile-to-brittle transition [7]. Efforts have been made to both explain and promote ductile regime cutting via modeling of material behavior with respect to the crystal structure [8], and by using assisted machining processes [9].

Among those efforts, workpiece surface coatings also enhance ductile cutting regime and thus process throughput in the machining of ceramics. The use of coatings is easier and cheaper than other procedures. Lee et al. used solidified ink coatings to calcium fluoride to suppress cracking [10], while Kalkhoran et al. applied hybrid (wax and oil) coatings to sapphire, which served as a chip breaker and lubricant [11]. However, the effects of coating properties on material behaviors and cutting forces are not yet well-understood. Lubrication [12] or

^{*} Corresponding author at: Department of Mechanical Engineering, University of Wisconsin-Madison, Room 1039, 1513 University Avenue, Madison, WI 53706, USA.

E-mail addresses: hsyoon7@kau.ac.kr (H.-S. Yoon), kwon47@wisc.edu (S.B. Kwon), jhkim96@kau.kr (J.-H. Kim), ahnsh@snu.ac.kr (S.-H. Ahn), sangkee.min@wisc.edu (S. Min).

application of hydrostatic pressure [10] can play important roles, but the effects of the various coating materials on cutting forces have received little attention. No optimum coating material has yet been identified.

Further, the machining characteristics of monocrystalline material vary greatly by the crystal orientation [13]. The dominant deformation/fracture mechanism during cutting was influenced by the magnitude and direction of the resultant cutting force, and the ductile cutting regime significantly varies in terms of crystal orientation. Attempts have been made to construct models for prediction of machining behaviors with respect to stress intensity factor [14] or fracture toughness and surface energy [15], as well as materials' crystallography. In the previous study [13], machining characteristics were analyzed with different cutting directions on different crystal planes. Thus, when evaluating coatings, both the coating material per se and the cutting orientation must be considered.

To this end, this study aims to explore and reveal the effects of coating materials on cutting forces and the material responses during ductile regime cutting. Various surface coatings, elastomers, hard coatings, and liquid lubricant were tested during orthogonal cutting of monocrystalline sapphire in different directions. It was hypothesized that types of coatings would influence the forces in different manners.

The effects of coating materials were discussed based on cutting and thrust force values, their ratio change, behaviors during the machining, and crack morphologies. The difference in ductile cutting regime per cutting direction was discussed based on the modified slip-fracture model, considering the crystal structure and deformation mechanisms of the material. Experimental results implied that most coatings were effective in promoting the ductile cutting regime, but the effects of coatings should be carefully considered with respect to material's crystallography.

Surface coating is strongly believed to be a breakthrough for effective processing of ceramics. It is expected that this research can contribute to the prediction of the material response during the cutting with surface coatings and the determination of the optimal coating with respect to various materials and cutting conditions.

2. Materials and methods

2.1. Preparation of surface coatings

Three different types of coatings were considered. The first type featured flexible elastomers with good resilience; these coatings can store deformation energy. The second type included harder materials that can resist the workpiece deformation. The last type was a liquid lubricant with a very low friction coefficient.

The elastomers included two types of polydimethylsiloxane (PDMS; Sylgard 184 A/B, Dow Corning Corp., USA) with different amounts of curing agent. The hard coatings were an instant adhesive (NV-020, Navimro Inc., Korea) and a wax (Shiftwax 7607, Nikka Seiko Co. Ltd., Japan). Cutting fluid (RustlickTM EDM-250, ITW, USA) served as the low-friction test material.

Flow coating (Fig. 1) was used to ensure uniform layer thickness inspired by [16]. Each coating material was added to a workpiece that was then hung vertically for >1 h. The coating material was spread by

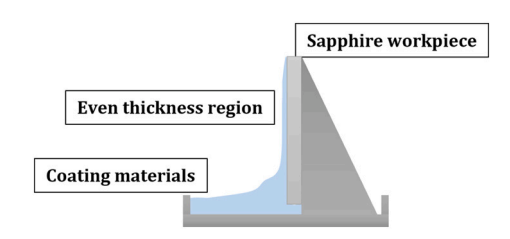


Fig. 1. A scheme of the coating process.

virtue of a gravitational force. Optical images of the rare sapphire wafer and coated surfaces are also available in Fig. S1. The thickness of the coating was measured at multiple points using a precise vernier caliper and the average thicknesses are listed in Table 1. Those coating thicknesses were the minimum thicknesses that could be achieved with the coating process. As the depth of cut (in the sapphire workpiece) is very small, the smaller coating thickness makes easier the cutting experiments. However, a longer duration (longer than 1 h) of the coating could not reduce the coating thickness anymore. Cutting fluid did not require a specific coating method.

Nanoindentations were then performed to measure the modulus and hardness of coated thin layers (Ultra nanoindentation tester, UNHT³, Anton Paar, Austria). A Berkovich tip was used to indent the coatings to depths of a few microns. The coating thickness may influence the mechanical properties of coatings, and Lee et al. [17] have utilized the effective coating hardness in terms of the thickness for the stress analysis. However, in this study, the effect of the coating thickness on mechanical properties did not significantly influence the basic material classifications, flexible polymer, and hard layer. With the given coating thickness and indentation depth, the measured mechanical properties of the PDMS layers showed a significant difference from the instant adhesive or wax layer. Table 2 lists the average values of measured mechanical properties of the coatings.

Sliding experiments were performed to acquire static friction coefficients (Fig. 2). The coatings were too thin and the adhesion between the coating and workpiece was too weak to allow scratch tests. The coated substrate was placed to make the coated surface contact another sapphire plate at the bottom. The bottom sapphire plate was then tilted until the substrate started to slide by the gravitational force. Friction coefficients were derived per different coating by calculating tangent values of the tilt angle when the substrate just started to slide.

2.2. Orthogonal cutting of monocrystalline sapphire

An ultra-precision machine tool (ROBONANO α-0iB, FANUC Corp., Japan) was used to perform orthogonal cutting on the C-plane of monocrystalline sapphire (iNexus Inc., Korea) employing a polycrystalline diamond tool with a nose radius of 500 µm (A.L.M.T. Corp., Japan). Fig. 3 shows the experimental configuration. A plunge cut with a slope of 1/500 was performed as the main cutting to observe the transition of predominant material behaviors from ductile to brittle in terms of the uncut chip thickness. Here, the coating thickness was controlled again before the main cutting. The top part of the coatings was machined by orthogonal cutting to leave coatings with a uniform thickness of about 2.5 μm on the workpiece for all cases. The main cutting was then performed to cut the coating and workpiece together as shown in Fig. 3 (b). A cutting speed of 5 mm min⁻¹ was applied to the main cutting with the maximum depth of cut of 1 μm . The maximum depth of cut was set based on the substrate. Although the coating thickness was higher than substrate cutting depth, the substrate cutting was confirmed with the known coating thickness and force measurement.

Cutting forces were captured by a dynamometer (Type 9119AA1, Kistler Instrument Corp., Switzerland) linked to a multi-channel amplifier (Type 5080A, Kistler Instrument Corp., Switzerland). The

Table 1The coating materials.

T	0	T all tolor
Types	Coating materials	Layer thickness
Elastomers	PDMS (10:1)*	30 μm
	PDMS (5:1)**	30 μm
Hard layers	Instant adhesive	10 μm
	Wax	10 μm
Liquid lubricant	Cutting fluids	_

^{*, **:} The ratio of the base to the curing agent. PDMS (10:1) is softer than PDMS (5:1) because the former contains the less curing agent.

Table 2 Mechanical properties of the coatings.

Coating	Elastic modulus	Hardness (Berkovich)	Friction
materials	[GPa]	[MPa]	coefficients
PDMS (10:1) PDMS (5:1) Instant adhesive	0.025 0.053 6.083	2.064 3.454 116.527	1.03 0.567 0.502
Wax	8.012	253.182	0.566
Cutting fluids	-	-	0.0087

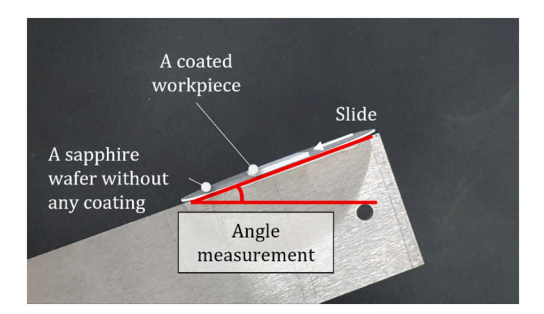


Fig. 2. A scheme of the sliding experiments.

sampling frequency was 20,000 Hz. A low pass filter with a cut-off frequency of 5000 Hz was applied to the signals. Owing to its high hardness, cutting sapphire was clearly distinguished from cutting surface coating in force signals. After cutting, the coating was removed, and the machined slots were observed using an optical microscope.

Fig. 4 shows an optical image of a slot. As a quantitative measure, the transition depth of cut, i.e., the uncut chip thickness at which the predominant material response changed from ductile to brittle, was measured by observing the machined surface where the crack begins to be appeared through optical images and cutting force signals like in the previous study [18]. Depth was a reasonable parameter that directly reflected the stress level and material removal rate. Though the transition depth of cut may vary with respect to detailed cutting conditions, the effects of coatings can be effectively compared from the perspectives of the depth, as all cuttings were performed using the same tool and process parameters.

2.3. The slip-fracture model

Monocrystalline sapphire exhibits anisotropic cutting characteristics because of its hexagonal unit-cell structure with three-fold symmetry [13]. Fig. 5 shows that cutting proceeded in the $[1\overline{1}00]$ and $[\overline{1}100]$ directions.

In the previous study, the modified slip-fracture model to describe material behavior was suggested [18]. The direction of the resultant force (F_R) is given below using the thrust force (F_t) and cutting force (F_c) , in terms of the unit direction vector (Fig. 6(a)).

$$\widehat{d}_{F_R} = \left(\cos\left\{\operatorname{atan}\left(\frac{F_t}{F_c}\right)\right\}\cos(\omega), \cos\left\{\operatorname{atan}\left(\frac{F_t}{F_c}\right)\right\}\sin(\omega), \sin\left\{\operatorname{atan}\left(\frac{F_t}{F_c}\right)\right\}\right)$$
(1)

where \widehat{d}_{F_R} is the unit vector of the resultant force direction, ω is the angle at which the resultant force is tilted from the *x*-axis, and $\tan\left(\frac{F_c}{F_c}\right)$ is the angle at which the resultant force is tilted from the cutting surface as shown in Fig. 6(a).

The plastic deformation parameter reflects the tendency of slip/twining activation and was then calculated as follows.

$$P_{i} = m_{i} / \left(\tau^{\text{crit}}_{i} / m_{i} n \tau^{\text{crit}}_{i}\right)$$
 (2)

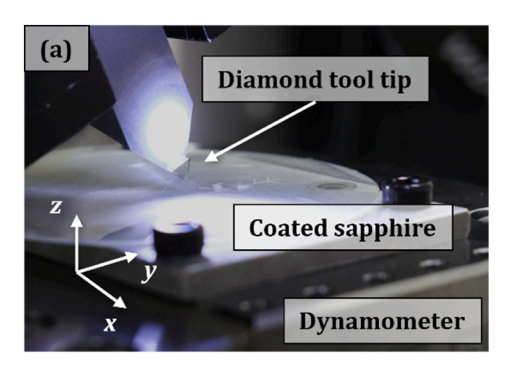
where P_i is the plastic deformation parameter, m_i is the modified Schmid factor reflecting the resultant force direction, and $\tau^{\rm crit}{}_i$ is the critical resolved shear stress for the i-th slip or twinning system as indicated in Table 3.

With the relationship between the crystal orientation and direction of resultant force during cutting, the predominant deformation mechanism can be predicted by comparing the tendency of each slip/twinning mechanism. $\tau^{\rm crit}_i$ is the given material property, and m_i can be calculated with a relationship between the slip/twinning and resultant force directions, or equal to $\cos(\theta_i)$ $\cos(\lambda_i)$. θ_i and λ_i are the angles between the plane normal of the i-th slip system and resultant force direction, and the angle between slip direction of the i-th slip system and resultant force direction respectively (Fig. 6(b)). For both cutting directions, rhombohedral twinning is a dominant plastic deformation mechanism, but in different directions (Fig. 5(b)).

The brittle fracture parameter reflects the tendency of crack propagation at given stress and was calculated as follows.

$$F_{j} = c_{j} / \left(K_{ICj} / \underset{j}{min} K_{ICj} \right) \tag{3}$$

where F_j is the brittle fracture parameter, c_j is the cleavage factor considering the resultant force angle, or equal to $\cos^2(\phi_j)$, and K_{ICj} is mode I critical stress intensity factor for the j-th fracture system as indicated in the Table 4. ϕ_j is the angles between the plane normal of the j-th fracture system and resultant force direction as shown in Fig. 6(c). Cracks propagate principally on the R-plane (the rhombohedral plane). In this study, those parameters were utilized to discuss the dominant deformation/fracture system with respect to the direction of the resultant cutting force. The brittle fracture parameters were calculated to further explain the varying effects of surface coating per different cutting directions.



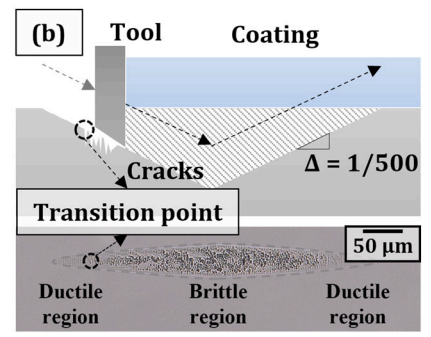


Fig. 3. Experimental configurations.

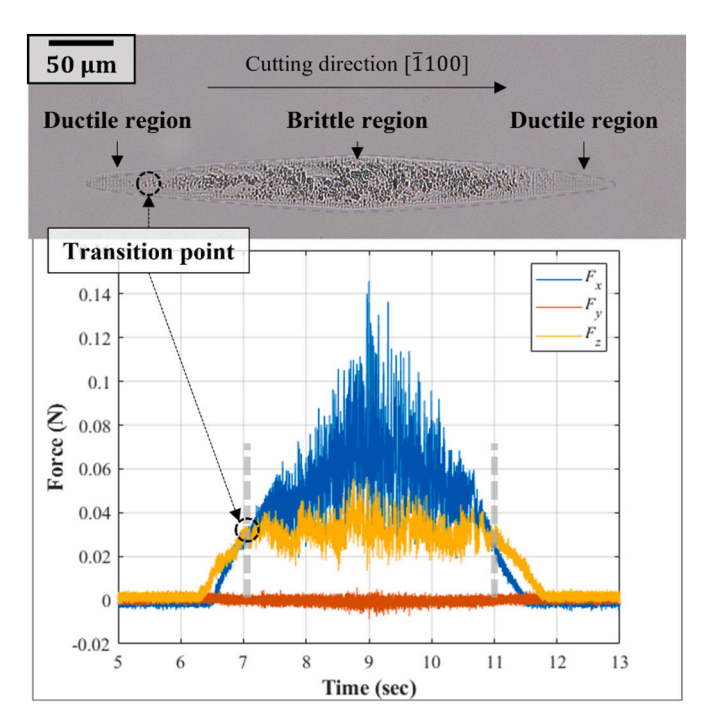


Fig. 4. An example of a machined slot and the definition of the transition point.

3. Results and discussion

3.1. Effects of the surface coatings on cutting forces

Fig. 7 compares the cutting and thrust forces at the transition depths of cut in $[1\overline{1}00]$ cutting direction. Compared to other coatings, the cutting fluid shows a very different thrust to cutting force ratio as reported in the literature [11] by inhibiting chip adhesion on the cutting edge. On the other hand, solid coatings generally showed higher thrust force than the original surface. The elastomer coatings (PDMS 10:1 and PDMS 5:1) reduced the cutting force (compared to the hard coatings) inferring that less force was required in the cutting direction for plastic deformation at the same depth. The instant adhesive and wax significantly increased thrust force.

High thrust-to-cutting force ratios of the surface coatings mean that additional downward force was applied to the material. As surface coatings resist the deformation of the workpiece and chip, more compressive stress was induced to the material, increasing the specific cutting energy [17]. The induced compressive stress stables slip deformation of the subsurface regions [10] and it is expected to promote the ductile cutting regime. To investigate the force characteristics per coating material in more detail, the thrust-to-cutting force ratios of some featured coatings were calculated in terms of the cutting depth (Fig. 8).

The elastomer coatings deformed readily and thus became compressed in front of the tool during machining. At a shallow cut depth (<200 nm), the deformation imparted an elastic force in the cutting direction and showed a larger cutting force and thus low thrust-to-cutting force ratio than those of the original surface as shown in Fig. 8. However, as the tool progressed, the size of the deformed region increased and became a circular shape (Fig. 9(a)). Due to elastomers' good resilience, it is thought that shear force was applied between the coating and the workpiece toward the radial direction following the deformed shape of the PDMS coating, creating shear stress components in the lateral direction.

The lateral shear stress was assumed to facilitate rhombohedral twinning on other R-planes ($(01\overline{1}2)$ and ($\overline{1}012$)). Enabling more deformation mechanisms could reduce energy dissipated in the cutting direction, reducing the cutting force compared to the hard coatings (Fig. 7). Since the internal accumulated stress energy could be released through the additional plastic deformation (rhombohedral twinning on other R-planes ($(01\overline{1}2)$ and ($\overline{1}012$))), the energy released in the cutting direction could be reduced. Thus, elastomer coatings can maintain high thrust-to-cutting force ratios even competitive to wax and can promote ductile cutting regime; the cracks would occur when the accumulated stress energy in the workpiece exceeds a certain threshold value. But the effects of the lateral stress components may vary with respect to the crystal orientation.

On the other hand, hard coating holds its position rather than deform. As the tool progressed, the thrust force increased significantly given the resistive force of the coating to the workpiece and chip (Fig. 9 (b)). The thrust-to-cutting force ratios remained higher than the original surface and elastomers owing to the coatings' high hardness (Fig. 8).

When compared to the instant adhesive, the wax coating was associated with high thrust-to-cutting force ratios at shallow cut depths ($<200\,$ nm), but the ratio rapidly decreased thereafter (Fig. 8). It is

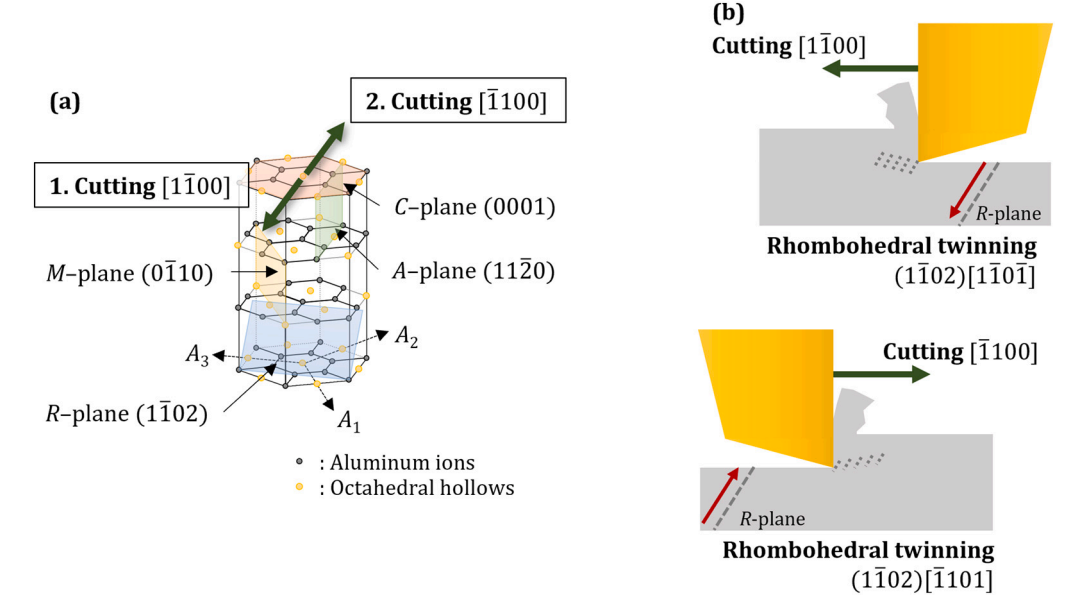


Fig. 5. (a) The crystal form of sapphire and (b) the different deformation directions in play at various cutting orientations.

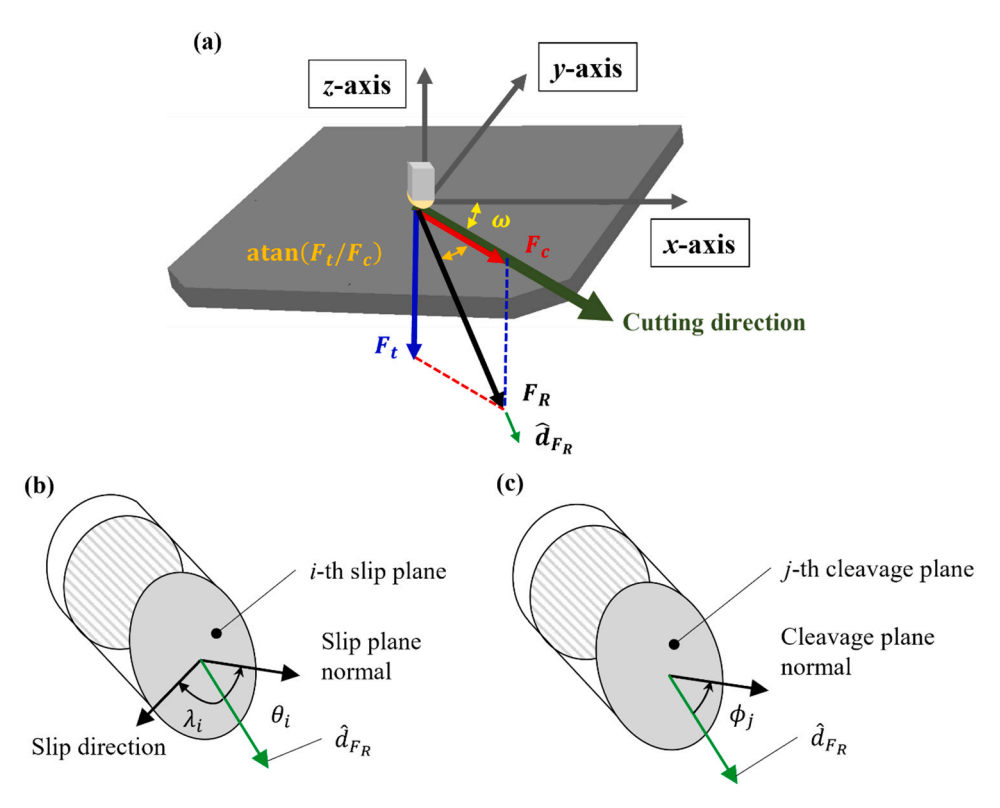


Fig. 6. Calculations of slip/fracture activation model. Calculation of (a) the direction of the resultant force during the machining, (b) resolved shear stress for plastic deformation parameters, and (c) resolved tensile stress for cleavage fracture parameters.

Table 3
Slip/twinning system of single-crystal sapphire [19].

Slip (twinning) system	Miller-Bravais indices	Critical resolved shear stress $(\tau^{\text{crit}}_{i}, \text{MPa})$
Basal twinning (C-plane) Basal slip (C-plane) Pyramidal slip Prismatic slip (A-plane) Rhombohedral twinning (R-plane)	$ \begin{array}{c} (0001) < \overline{1}010> \\ (0001) < 11\overline{2}0> \\ (0\overline{1}11) < 10\overline{1}1> \\ \{1\overline{1}\overline{2}0\} < \overline{1}100> \\ \{1\overline{1}02\} < 1\overline{1}0\overline{1}> \end{array} $	2.2255 2.2255 4.4817 1.6487 0.4066

Table 4Fracture system of single-crystal sapphire [20].

Fracture system	Miller-Bravais indices	Critical stress intensity factor $(K_{ICj}, \text{MPa·m}^{-\frac{1}{2}})$
Basal fracture (C-plane)	(0001)	4.54
Prismatic fracture (M- plane)	$\{10\overline{1}0\}$	3.14
Rhombohedral fracture (R-plane)	$\{\overline{1}012\}$	2.38
Prismatic fracture (A- plane)	$\{11\overline{2}0\}$	2.43

suggested that the higher friction than the instant adhesive increased the cutting force. Unlike the elastomers, the wax layer in contact with the tool did not exhibit large elastic deformation. As the tool progressed, the contact area increased, as did the friction between the tool and the wax. Despite the high thrust force (attributable to the high hardness), the thrust-to-cutting force ratio decreased even faster than that of the instant adhesive.

Nevertheless, all solid coatings showed higher thrust-to-cutting force ratios than the original surface and promoted the ductile cutting regime

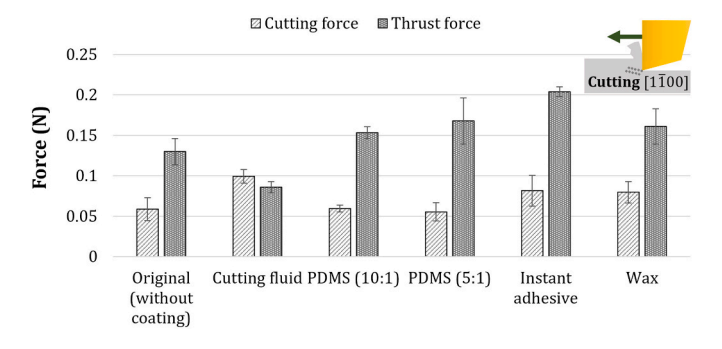


Fig. 7. Cutting force components at the transition depths of cut in the $[1\overline{1}00]$ direction (*C*-plane).

in [1100] direction (Fig. 10). Larger thrust forces in cutting with coatings imply that additional downward force was induced by the resistance of the coatings. Increases in compressive stresses in the primary deformation zone are beneficial to suppressing cracks [17] as mentioned above. It is not easy to say that the thrust-to-cutting force ratio is directly related to crack opening owing to the complex slip-fracture mechanisms of sapphire, but within the given experimental range, the thrust-to-cutting force ratios all decreased as the cutting proceeded and reached the brittle region (Fig. 8). The instant adhesive afforded the highest transition depth of cut owing to its highest thrust-to-cutting force ratio, then followed by the wax, PDMS (5:1), and PDMS (10:1). Compared to the original surface (without any coating), the improvement was about 40 %. Considering that control of tool posture or cutting speed improved the transition depth of cut by about 40–50 % [21], surface coatings can improve the ductile cutting regime competitively.

Some optical image examples of machined slots are provided in Fig. S2. Although the types of coatings influence the forces in different manners, both elastomers and hard coatings increased the thrust-to-

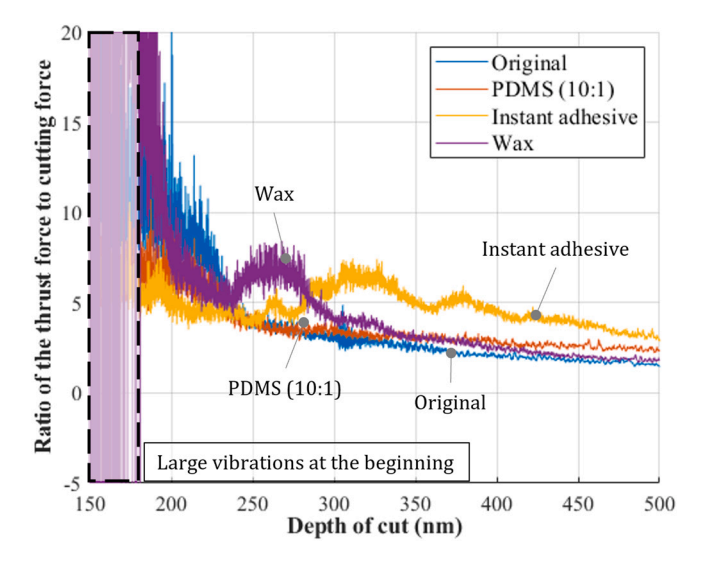


Fig. 8. Thrust to cutting force ratios in terms of cutting depth.

cutting force ratios and transition depth of cuts. The results also showed an agreement with the research by Lee and Wang [22]. The authors of the above literature utilized the epoxy coating in the machining of calcium fluoride and claimed that the deformation of coating induces a reaction force back into the work material and analyzed the stress distribution with respect to the crystal orientation. However, in this research, the crack morphologies did not change whether the coating was applied or not, as the dominant crack opening mechanisms did not change.

3.2. Effect of crystal orientation on the ductile cutting regime

To confirm the suggested effects of the various coatings, cutting was

next performed in the opposite direction [$\overline{1}100$]. Fig. 11 shows the cutting and thrust forces at the transition depth of cut, and Fig. 12 shows the transition depth of cut data when cutting in the [$\overline{1}100$] direction. Some optical image examples of machine slots are provided in the supplementary material (Fig. S3). Elastomer coatings were associated with a lower cutting force compared to hard coatings, and hard coatings showed higher thrust forces than elastomer coatings, as expected in the former section. The crack morphologies still did not change with respect to the coating types.

Despite similar cutting force behaviors, the effects of the coatings on the transition depth of cut were larger in this direction. When compared to Fig. 10, the improvements of the transition depth of cut (from the original surface) were much higher in Fig. 12. Crystal orientation influences the effects of surface coatings. Compared to the $[1\overline{1}00]$ direction, the direction of the resultant force is closer to the *R*-plane normal (the dominant crack opening plane) in the $[\overline{1}100]$ direction (Fig. 13(a)). It is thus thought that maintaining a high thrust-to-cutting force ratio is

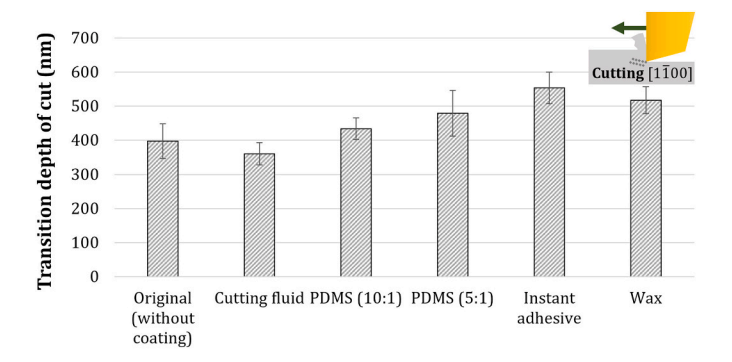


Fig. 10. Average transition depth of cuts in the $[1\overline{1}00]$ direction of the *C*-plane of sapphire.

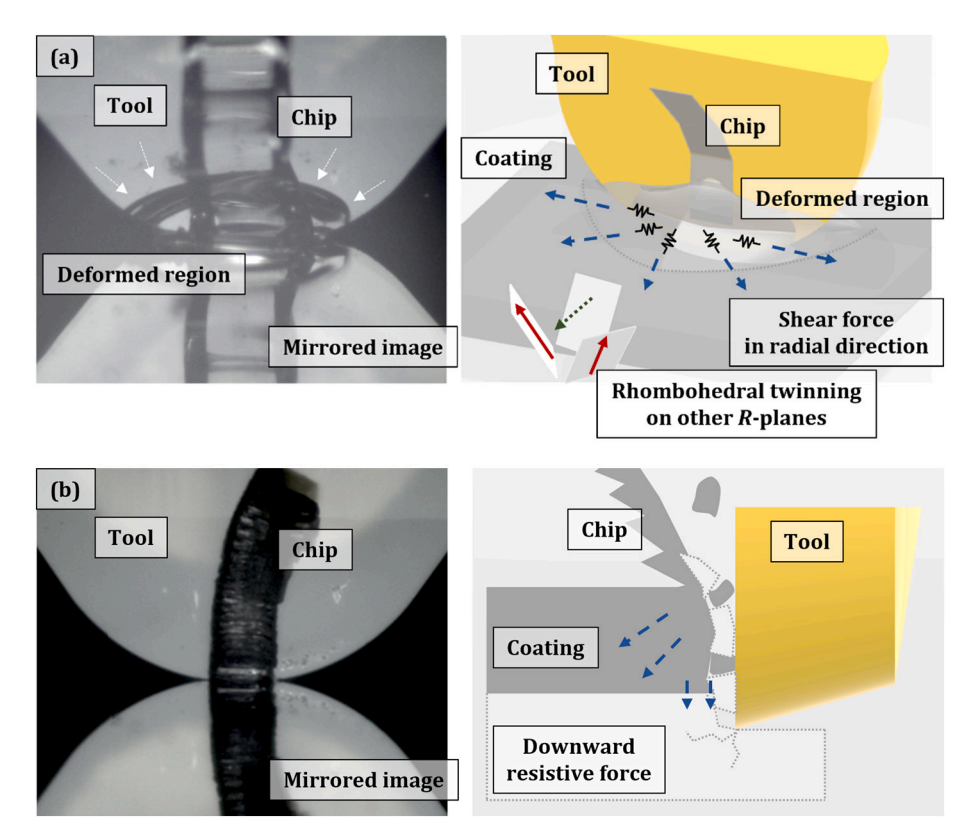


Fig. 9. The effects of (a) elastomers and (b) a hard coating on force behaviors during cutting, with optical images captured during cutting.

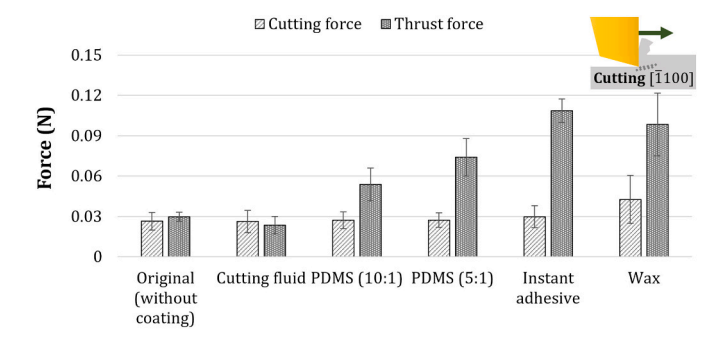


Fig. 11. Cutting force components at the transition depths of cut in the $[\overline{1}100]$ direction (*C*-plane).

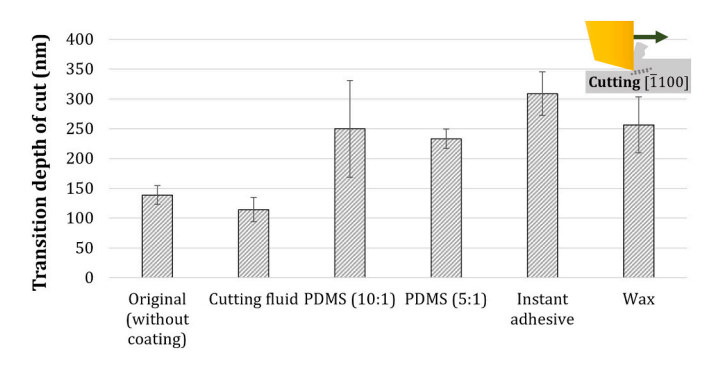


Fig. 12. Transition depth of cuts in the $[\overline{1}100]$ direction of the *C*-plane of sapphire.

more effective in this cutting direction to enhance the ductile cutting regime. For example, in the $[\overline{1}100]$ direction, a high thrust-to-cutting force ratio can more effectively reduce the force components in $[1\overline{1}02]$ direction, the R-plane normal direction, or suppress force components contribute to the crack opening.

Further, elastomer coatings showed higher improvement rates in the transition depth of cut in this direction, even competitive to wax coating (Fig. 12). Fig. 13(b) shows the plastic deformation parameters from rhombohedral twinning on other *R*-planes ((01 $\overline{1}$ 2) and ($\overline{1}$ 012)) with estimated lateral stress components. Compared to cutting in [1 $\overline{1}$ 00] direction, rhombohedral twinning on other *R*-planes can be activated easier with given cutting forces. The effect of enhanced plastic deformation parameters becomes larger in this cutting direction and was thought to improve the transition depth of cut.

Although the high thrust-to-cutting force ratio showed a high transition depth of cuts in the experiments, it is not easy to exactly match the transition depth of cut and the thrust-to-cutting force ratio. Cutting forces influence the crack propagation on various crystal planes simultaneously. To consider the tendency of crack propagation, the brittle fracture parameters calculated based on the resultant forces was shown in Fig. 14. Coatings reduced the brittle fracture parameters compared to the original surface and thus improved the transition depth of cut. The instant adhesive showed the highest transition depth of cut owing to the lowest brittle fracture parameter, and wax and PDMS (10:1) coatings showed similar transition depth of cuts (Fig. 12). The brittle fracture parameter could compare fracture tendency under the same cutting conditions, but with different surface coatings.

In summary, the hard coatings were more effective than the elastomers when cutting in the $[1\overline{1}00]$ direction, but the elastomers were also competitively effective during cutting in the $[\overline{1}100]$ direction, inferring the existence of shear stress in a lateral direction. Hard coatings increased the thrust force by the resistance of the coating to the workpiece and chip, expected to induce compressive stress to the workpiece.

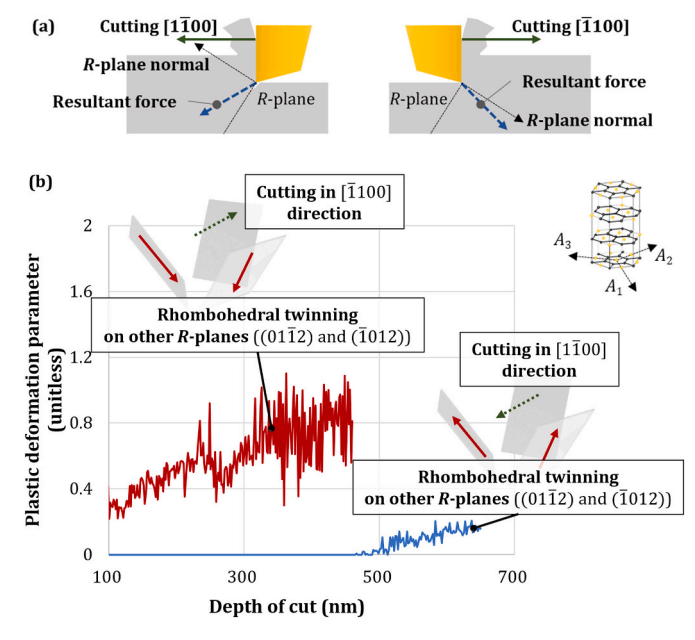


Fig. 13. (a) Comparison of the effects of the resultant forces in different cutting directions and (b) the plastic deformation parameters of rhombohedral twinning on *R*-planes ($(01\overline{1}2)$ and ($\overline{1}012$)) affected by different cutting directions.

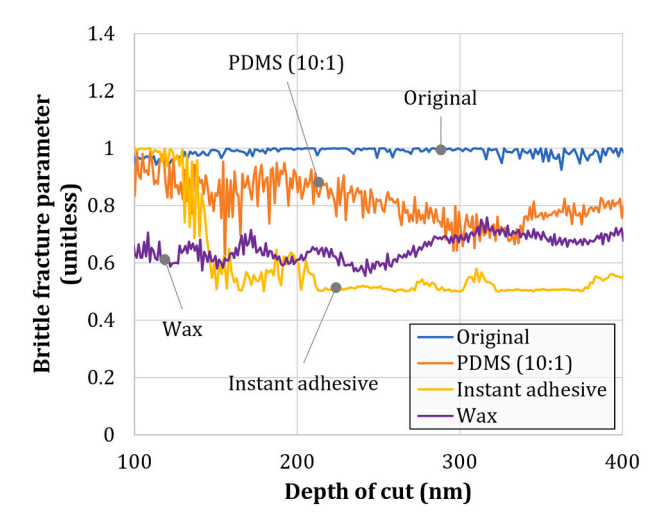


Fig. 14. The brittle fracture parameters calculated with measured cutting forces in the $[\bar{1}100]$ direction (*C*-plane).

The effects of surface coating on cutting forces also showed anisotropy with respect to relevant deformation/fracture mechanisms.

A detailed numerical analysis will follow to simulate crack opening and propagation with various types of coating. The surface coating can also change crack morphologies as well as the stress distribution. The coating process and thickness will be further optimized; Lee and Tan claimed that the coating thickness influenced the ductile-to-brittle transition, and further increment of the coating thickness might not be effective [23]. As the current coating thicknesses are higher than the cutting depth in sapphire, thinner coatings will be investigated using other processes such as spin coating. It is expected that the surface coating can contribute to the understanding of ductile-to-brittle transition in the machining of ceramic materials as well as effective process improvements.

4. Conclusion

The effects of coating materials on the ductile cutting regime were investigated in the machining of monocrystalline sapphire. These materials influenced the force components differently and increased the thrust-to-cutting force ratio. The increased ratio here suppressed cracking and promoted the ductile regime cutting. However, their effects varied by cutting orientation. The improvement ratio of the ductile cutting regime varies regardless of the original value (without coating), despite similar thrust-to-cutting force ratios; Elastomer coatings showed similar improvements to hard coatings in one direction. The effects of affected cutting forces were explained in more detail based on the slip-fracture model.

Here, coatings were applied with the flow coating method. Without precise control of coating thickness or expensive coaters, coatings could be easily applied to a large area and were effective in promoting the ductile cutting regime. It is believed that surface coatings would be widely utilized in the industries. It is expected that this research can contribute to the development of user assistant tools to select proper coating with respect to materials with different deformation mechanisms and cutting conditions. If an appropriate coating is selected, the ductile cutting regime can be significantly enhanced, aiding the effective processing of ceramic materials.

Declaration of competing interest

The authors declare that they have no known competing financial interests or personal relationships that could have appeared to influence the work reported in this paper.

Acknowledgement

This work was supported by the National Research Foundation of Korea (NRF) grants (Nos. NRF-2022R1F1A1063896, 5199990714521, 2021R1A4A2001824, and 2021R1A2B5B03087094), 2020 Korea Aerospace University Faculty Research Grant, National Science Foundation (NSF) grant (No. CMMI-1844821), kind support from FANUC Corporation, Japan, for the loan of 5-axis ultra-precision machine tool, ROBONANO $\alpha\text{-}0iB$, and from A.L.M.T. Corporation, Japan, for providing the discounted diamond tools used in this study.

Appendix A. Supplementary data

Supplementary data to this article can be found online at https://doi.org/10.1016/j,jmapro.2022.09.046.

References

- Liu Y, Deng J, Yue H, Duan R, Li X, Ehmann K. Material removal behavior in processing green Al2O3 ceramics based on scratch and edge-indentation tests. Ceram Int 2019;45(9):12495–508. https://doi.org/10.1016/j. ceramint.2019.03.185.
- [2] Huang S, Li X, Zhao Y, Sun Q, Huang H. A novel lapping process for single-crystal sapphire using hybrid nanoparticle suspensions. Int J Mech Sci 2021;191:106099. https://doi.org/10.1016/j.ijmecsci.2020.106099.

- [3] Yoon H-S, Kwon SB, Nagaraj A, Min S. Effect of the initial-flaw on crack-propagation in two-step cutting of monocrystalline sapphire. J. Manuf. Process. 2020;56/A:1211–8. https://doi.org/10.1016/j.jmapro.2020.06.017.
- [4] Wang Y, Liang Z, Zhao W, Wang X, Wang H. Effect of ultrasonic elliptical vibration assistance on the surface layer defect of M-plane sapphire in microcutting. Mater Des 2020;192:108755. https://doi.org/10.1016/j.matdes.2020.108755.
- [5] Wan L, Li L, Deng Z, Deng Z, Liu W. Thermal-mechanical coupling simulation and experimental research on the grinding of zirconia ceramics. J Manuf Process 2019; 47:41–51. https://doi.org/10.1016/j.jmapro.2019.09.024.
- [6] Davies MA, Owen JD, Troutman JR, Barnhardt DL, Suleski TJ. Ultra-precision diamond machining of freeform optics. Imaging and Applied Optics 2015;2015: FM1B.1. https://doi.org/10.1364/FREEFORM.2015.FM1B.1.
- [7] Zhang T, Jiang F, Huang H, Lu J, Wu Y, Jiang Z, Xu X. Towards understanding the brittle-ductile transition in the extreme manufacturing. Int J Extreme Manuf 2021: 3/2:022001. https://doi.org/10.1088/2631-7990/abdfd7.
- [8] Lucca DA, Klopfstein MJ, Riemer O. Ultra-precision machining: cutting with diamond tools. J Manuf Sci Eng 2020;142/11:110817. https://doi.org/10.1115/ 1.4048194.
- [9] Yang Z, Zhu L, Zhang G, Ni C, Lin B. Review of ultrasonic vibration-assisted machining in advanced materials. Int J Mach Tool Manuf 2020;156:103594. https://doi.org/10.1016/j.ijmachtools.2020.103594.
- [10] Lee YJ, Chong JY, Chaudhari A, Wang H. Enhancing ductile-mode cutting of calcium fluoride single crystals with solidified coating. Int J Precis Eng Manuf -Green Technol 2019;7:1019–29. https://doi.org/10.1007/s40684-019-00126-0.
- [11] Kalkhoran SNA, Vahdati M, Zhang Z, Yan J. Influence of wax lubrication on cutting performance of single-crystal silicon in ultraprecision microgrooving. Int J Precis Eng Manuf - Green Technol 2021;8:611–24. https://doi.org/10.1007/s40684-020-00198-3
- [12] Yang M, Li C, Zhang Y, Jia D, Zhang X, Hou Y, Li R, Wang J. Maximum undeformed equivalent chip thickness for ductile-brittle transition of zirconia ceramics under different lubrication conditions. Int J Mach Tool Manuf 2017;122:55–65. https:// doi.org/10.1016/j.ijmachtools.2017.06.003.
- [13] Yoon H-S, Kwon SB, Nagaraj A, Lee S, Min S. Study of stress intensity factor on the anisotropic machining behavior of single crystal sapphire. CIRP Ann 2018;67(1): 125–8. https://doi.org/10.1016/j.cirp.2018.04.114.
- [14] Yang M, Li C, Zhang Y, Jia D, Li R, Hou Y, Cao H. Effect of friction coefficient on chip thickness models in ductile-regime grinding of zirconia ceramics. Int J Adv Manuf Technol 2019;102:2617–32. https://doi.org/10.1007/s00170-019-03367-0
- [15] Huang W, Yu D, Zhang M, Cao Q, Yao J. Predictive cutting force model for ductile-regime machining of brittle materials. Int J Adv Manuf Technol 2018;98:781–90. https://doi.org/10.1007/s00170-018-2273-6.
- [16] Stafford CM, Roskov KE, Epps III TH, Fasolka MJ. Generating thickness gradients of thin polymer films via flow coating. Rev Sci Instrum 2006;77:023908. https://doi. org/10.1063/1.2173072.
- [17] Lee YJ, Kumar S, Wang H. Beneficial stress of a coating on ductile-mode cutting of single-crystal brittle material. Int J Mach Tools Manuf 2021;168:103787. https://doi.org/10.1016/j.ijmachtools.2021.103787.
- [18] Kwon SB, Nagaraj A, Yoon H-S, Min S. Study of material removal behavior on R-plane of sapphire during ultra-precision machining based on modified slip-fracture model. Nanotechnol Precis Eng 2020;3:141–55. https://doi.org/10.1016/j.npe.2020.07.001.
- [19] Clayton JD. A continuum description of nonlinear elasticity, slip and twinning, with application to sapphire. Proc R Soc Lond A Math Phys Sci 2008;465:307–34. https://doi.org/10.1098/rspa.2008.0281.
- [20] Iwasa M, Bradt RC. Fracture toughness of single-crystal alumina. Adv Appl Ceram 1984;10:767–79.
- [21] Yoon H-S, Kwon SB, Nagaraj A, Min S. Investigation of the ductile cutting behavior of monocrystalline yttria-stabilized zirconia during ultra-precision orthogonal cutting. Int J Precis Eng Manuf 2019;20(9):1475–84. https://doi.org/10.1007/ s12541-019-00150-9.
- [22] Lee YJ, Wang H. Characterizing crack morphology toward improving ductile mode cutting of calcium fluoride. Ceram Int 2021;47(20):28543–56. https://doi.org/ 10.1016/j.ceramint.2021.07.012.
- [23] Lee YJ, Tan RT. Compression effects of epoxy coating in microcutting of calcium fluoride single crystals. In: Euspen's 20th international conference & exhibition, Geneva, CH, June; 2020.